EXPLOSION SOURCE MODEL DEVELOPMENT IN SUPPORT OF SEISMIC MONITORING TECHNOLOGIES: NEW MODELS ACCOUNTING FOR SHOCK-INDUCED TENSILE FAILURE

Howard J. Patton

Los Alamos National Laboratory

Sponsored by National Nuclear Security Administration

Contract No. DE-AC52-06NA25396

ABSTRACT

The traditional source model for long-period seismic waves from nuclear explosions consists of a monopole releasing tectonic strain. Tectonic release has been studied since the 1960’s, and numerous studies have shown that linear superposition of monopole + double-couple sources can explain many observations of Rayleigh and Love waves. Free surface interactions and the dynamics of shock-wave rebound are responsible for modes of tensile failure which can also lead to permanent deformations affecting long-period excitation. Indeed, the vast majority of nuclear explosions worldwide were conducted under containment conditions that facilitated shock-induced, deep-seated tensile failure. A new source model, which is a superposition of monopole + tectonic release + shock-induced tensile failure, is proposed, the latter source represented by a compensated-linear-vector dipole (CLVD) with vertical axis of symmetry. This CLVD source does not excite Love waves. I draw upon the Toksöz-Kehrer (1972) model for tectonic release where F is an index measuring long-period source strength of the release relative to monopole moment M_I. A new index K, analogous to F, is introduced, providing a relative measure of M_{CLVD}, the source strength of tensile failure. M_{CLVD} vanishes for $K = 1$, and is > 0 in the case of extensional deformation along the vertical axis, e.g., $K > 1$.

Rayleigh waves from the CLVD destructively interfere with waves from the monopole, and polarity reversals occur on all azimuths for $K >$ ~3 in Poisson media. Most Nevada Test Site (NTS) observations support ~1 < K < 3, and as such the new model predicts lower M_s compared to the traditional model involving just tectonic release. This effect of tensile failure on M_s improves m_b - M_s discrimination and suggests that anomalously large M_s compared to m_b for the North Korean test of 9 October 2006 is due to the absence of tensile failure on this explosion.

Report Documentation Page

Form Approved
OMB No. 0704-0188

1. REPORT DATE	2. REPORT TYPE	3. DATES COVERED
SEP 2008		**00-00-2008 to 00-00-2008**

4. TITLE AND SUBTITLE	
Explosion Source Model Development in Support of Seismic Monitoring Technologies: New Models Accounting for Shock-Induced Tensile Failure	5a. CONTRACT NUMBER
	5b. GRANT NUMBER
	5c. PROGRAM ELEMENT NUMBER
6. AUTHOR(S)	5d. PROJECT NUMBER
	5e. TASK NUMBER
	5f. WORK UNIT NUMBER
7. PERFORMING ORGANIZATION NAME(S) AND ADDRESS(ES) **Los Alamos National Laboratory,PO Box 1663,Los Alamo,NM,87545**	8. PERFORMING ORGANIZATION REPORT NUMBER
9. SPONSORING/MONITORING AGENCY NAME(S) AND ADDRESS(ES)	10. SPONSOR/MONITOR'S ACRONYM(S)
	11. SPONSOR/MONITOR'S REPORT NUMBER(S)

12. DISTRIBUTION/AVAILABILITY STATEMENT

Approved for public release; distribution unlimited

13. SUPPLEMENTARY NOTES

Proceedings of the 30th Monitoring Research Review: Ground-Based Nuclear Explosion Monitoring Technologies, 23-25 Sep 2008, Portsmouth, VA sponsored by the National Nuclear Security Administration (NNSA) and the Air Force Research Laboratory (AFRL)

14. ABSTRACT

see report

15. SUBJECT TERMS

16. SECURITY CLASSIFICATION OF:			17. LIMITATION OF ABSTRACT	18. NUMBER OF PAGES	19a. NAME OF RESPONSIBLE PERSON
a. REPORT	b. ABSTRACT	c. THIS PAGE			
unclassified	**unclassified**	**unclassified**	**Same as Report (SAR)**	**9**	

Standard Form 298 (Rev. 8-98)
Prescribed by ANSI Std Z39-18

OBJECTIVE

The objective is to develop new analytical explosion source models based on seismic moment tensor theory for further improvement and advancement of regional seismic discrimination and yield-estimation technologies. Such technologies rely heavily upon the source information contained in high-frequency shear (*S*) waves. The use of coda waves following regional *S* phases to estimate explosion yield is one example of an emerging technology offering great promise for improved nuclear monitoring. Unfortunately, an understanding of how explosions excite *S* waves is quite limited, and a widening gulf between theory and practice undermines our confidence to monitor broad areas at small yields. The new models will provide a physical basis for explosion-generated *S* waves and theoretical insights for advancing yield estimation and discrimination capabilities, thereby closing the gulf between theory and practice.

RESEARCH ACCOMPLISHED

This project builds upon spherical (monopole) explosion source models developed in the 1970's. An important aspect of these models is the theory relating seismic amplitudes (in this case only compressional waves) directly to yield, depth of burial, and material properties of the source medium. Analytical relationships predicted by the theory draw upon empirical yield-scaling behaviors of key model constructs, such as the elastic radius. Furthermore, the analytical nature of these models facilitated their use since they were easy to implement by researchers, and as such they were widely applied to study the explosion source. Their application continues to this day, but with the recognition that a spherical point source is inadequate to explain *S*-wave generation.

Tensile failure is a source of asymmetry known to exist on most underground explosions, even those overburied for their yield. A kinematic description of shock-induced, deep-seated tensile failure is a CLVD with a vertical axis of symmetry in extension. A CLVD can generate *S* waves directly and indirectly through efficient excitation of short-period surface waves (Rg) and subsequent scattering into *P* and *S* waves close to the source. The research conducted in this project will introduce this source of asymmetry into spherical source models. The new model will require the development of scaling relationships like those for the elastic radius in the case of the spherical model, but for parameters of the tensile failure source, including centroid depth, source process time, and strength of the CLVD force system. A simple analytical form couched in seismic moment tensor theory will be adopted so that the model can be easily incorporated into researchers' preferred wave propagation codes for calculating synthetic seismograms.

In this first year of funding, the approach to model development was to start with a long-period description, such that a point-source approximation and step-function time dependence is valid. Rayleigh wave excitation was studied for an explosion source model involving a superposition of monopole, tensile failure, and tectonic release point sources. The relative strength of the CLVD compared to the monopole is given by an index *K*. Long-period Rayleigh wave amplitudes are reduced owing to destructive interference between an explosive monopole and a CLVD source with a vertical axis of symmetry in extension. The effect of tensile failure on M_s is to enhance the explosion-like characteristics on a plot of m_b - M_s. This model suggests that the m_b - M_s discriminant is so successful owing to the fact that nuclear tests were conducted under containment practices for which tensile failure is ubiquitous. The North Korean nuclear test of 9 October 2006 is a harbinger of poor m_b - M_s performance when tensile failure is suppressed. This work was submitted and accepted for publication in *Geophysical Research Letters* (Patton and Taylor, 2008).

Inferred K for NTS explosions and comparisons with measured K values. The *K* value is defined as follows

$$K = \frac{2M_{zz}}{M_{xx} + M_{yy}} \quad \text{or} \quad \frac{M_{CLVD}}{M_I} = \frac{2(K-1)}{K+2} \quad , \qquad (1)$$

where M_{ii} are diagonal elements of the moment tensor, M_{CLVD} is the moment of the CLVD source and M_I is the monopole moment (see Patton and Taylor, 2008, for details). Note that M_{CLVD} equals 0 for K equal to 1. The Rayleigh-wave reduced excitation spectrum $A(\omega)$ (Patton, 1988) is of interest and serves as a surrogate for network-averaged M_s,

$$A(\omega) = (M_{xx} + M_{yy}) \cdot G_1(\omega) + M_{zz} \cdot G_2(\omega) \quad , \qquad (2)$$

where G_1 and G_2 are Greens functions and ω is the angular frequency. The degeneracy of long-period Rayleigh wave Greens functions for shallow sources is well known (*c.f.*, Patton, 1988):

$$G_2(\omega) \rightarrow -(2\nu/(1-\nu)) \cdot G_1(\omega) , \qquad (3)$$

where ν is Poisson ratio. For a Poisson solid ($\nu = 1/4$),

$$G_2(\omega) \rightarrow -2/3 \cdot G_1(\omega) . \qquad (4)$$

A low-frequency approximation of $A(\omega)$ in terms of the new source model is

$$A(\omega) \sim f(K) \cdot M_I \cdot G_1(\omega) \quad , \qquad (5)$$

where $f(K) = 6 \cdot (1 - \nu - K\nu)/(2 + K)(1 - \nu)$. (6)

A CLVD with a vertical axis of symmetry in tension radiates Rayleigh waves uniformly in all azimuths just as the monopole does, but with opposite polarity. Destructive interference occurs between the sources for $K > 1$, constructive interference for $K < 1$. As K increases above 1, Rayleigh-wave amplitudes decrease until K reaches a value of 3 in a Poisson solid at which point polarity reversals occur at long-periods; amplitudes begin to increase for larger K values. This CLVD source does not radiate Love waves.

Patton (1988) applied a method due to Romanowicz (1982) for decomposing Rayleigh-wave amplitude and phase observations into five azimuthal constituents (1, cosθ, sinθ, cos2θ, sin2θ) of the radiation pattern. The A spectrum is extracted from the azimuth(θ)-independent constituent. Ekström and Richards (1994) employed a relative spectrum approach for explosion sources located in a small area and exploited the fact that low-frequency Greens functions vary little over plausible burial depths. This approach reduces the spectrum for different explosions to a scalar representing a gain factor with respect to an empirically-derived template $A_t(\omega)$. Figure 1 plots the logarithm of the gain factor logA' against m_b for 67 explosions, the vast majority located on Pahute and Rainier Mesas, recorded on seismic networks operated by Livermore and Sandia National Laboratories. The m_b values are averages determined from regional and teleseismic estimates of $m_b(Pn)$ and $m_b(P)$.

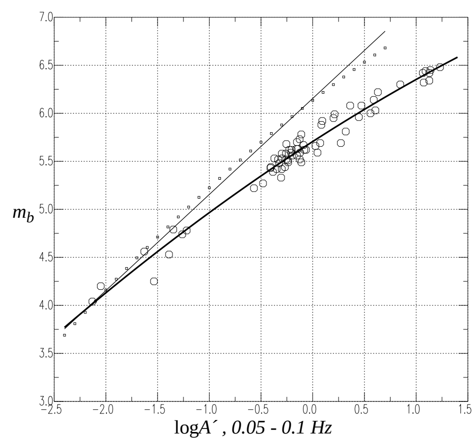

Figure 1. LogA' versus m_b for 67 NTS explosions. Solid line is fit to observations. Dots are amplitudes measured off *RDP* for tuff medium, and thin line has a slope of 1.0.

Observations in Figure 1 were subjected to regression analysis, and a quadratic model gave the best fit to the curvature or roll-over with increasing yield. The roll-over is not predicted by the Mueller-Murphy model (Mueller and Murphy, 1971; MM71), as shown in the figure for calculations based on a reduced displacement potential (*RDP*) in tuff. These calculations were tied to the observations by assigning *RDP* amplitudes measured around 0.05 and 1 Hz for a 1-*kt* explosion log*A´* and m_b values of –2.1 and 4.05, respectively. MM71 predicts m_b and M_s scale close to 1:1 for yields less than ~1 *Mt*.

The simple relationship between the *A* spectrum and source parameters, M_I and *K*, in Equation 5 above raises the question, what inferences about the source and a dependence of *K* on yield *W* can be made concerning the roll-over. To this end, I turned to fundamental source theory and the scaling results of Denny and Johnson (1991;DJ91). The interested reader is referred to the paper by Patton and Taylor (2008) for details. Very briefly, we deduced the general form of *K*'s dependence on yield for NTS explosions as follows: (a) adopted DJ91's formulas for M_I (involves Equations 39 and 41 in their paper), (b) assumed nominal values for source region velocity, density, and gas porosity, and a nominal containment practice (e.g., depth of burial = $120 \cdot W^{1/3}$) for use in those formulas, (c) utilizing computed Greens functions for a Pahute Mesa velocity model, estimated the seismic moment of the empirical template used to obtain gain factors, and finally (d) adopted the m_b-*W* formulas of Vergino and Mensing (1990). Perturbations of the m_b-*W* formula for Pahute Mesa were tried, and in all cases the same general behavior of *K* was obtained.

The results are plotted in Figure 2 along with measurements of *K* values for 67 NTS explosions obtained from moment tensor inversions of regional data following the method of Patton (1988, 1991). The inferred yield dependence of *K* closely matches the measurements; however, the *K* values are too high, especially for m_b > 5.0. If the intercept of the m_b-*W* formula is larger than Vergino and Mensing's estimate, the fit to the measurements improves. There are other possibilities why the inferred *K* values are too high which are currently under investigation. The measured *K* values have large error bars, and work is underway to improve the moment tensor inversion method in order to reduce the error.

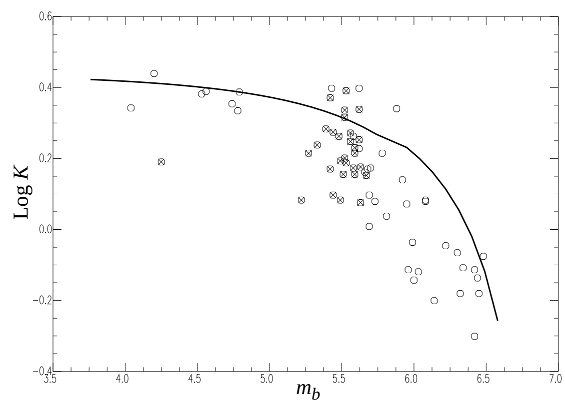

Figure 2. Inferred dependence of *K* on m_b (or yield; solid line) and measured *K* from moment tensor inversions. Twenty-nine Pahute Mesa tests above the water table are plotted with a circle-enclosed ×.

For m_b above 5.6, the rapid decrease in *K* suggests a connection with improved coupling for water-saturated shots. Shock waves impinging on the free surface are more forceful for shots below the water table, and spall mass and velocities increase dramatically compared to shots above, as empirical scaling relations for spall impulse show (Patton, 1990). *K* decreasing with yield may be telling us that the force of slapdown causes more compaction of the tuff matrix, closing voids, and reducing the static deformation of the CLVD source as yield increases. By the time yields reach 0.5-1 *Mt*, the deformation associated with deep-seated tensile failure is reduced to nearly zero. Kinematically speaking, the largest NTS explosions look virtually isotropic if the effects of tectonic release are ignored.

Most of the explosions with m_b less than 5.0 in Figure 2 are located on Rainier Mesa and have emplacement depths somewhat deeper for their yield compared to explosions on Pahute Mesa. It is interesting that their measured *K* values are among the largest, even though "intuition" says that M_{CLVD} should become smaller for explosions of a set yield as depth-of-burial increases. Individual measurements in Figure 2 are tentative until moment tensor inversion techniques are improved to reduce the measurement error on an event-by-event basis. Still, the tendency for *K* to increase with scaled depth-of-burial (SDOB) for a number of overburied explosions suggests it might be real.

It is important to acknowledge the limits of our understanding of the phenomenology of tensile failure and the behavior of *K* as a function of SDOB. There is no argument that *K* must approach 1 as SDOB gets very large. Nevertheless, physical reasons may exist for *K* to increase over a certain range of SDOB before it starts to decrease.

While spallation per se is not the focus of the new source model, gravitational unloading of surface layers is a facilitator of shock-induced tensile failure at depth. Spallation and deep-seated tensile failure are remarkably robust phenomena, and observations suggest that the range where *K* decreases occurs at surprisingly large values of SDOB. For example, the 550 m 25-ton Balapan chemical explosion on 28 September 1997 with an SDOB of ~1450 scale meters did in fact spall, and has a *K* value of 1.1 (Patton et al., 2005). The 300-m 25-ton chemical explosion on 31 August 1997 with an SDOB of 770 also spalled and has a *K* value of 1.6. The change in *K* for these two shots fits intuition: *K* approaches 1 for very large SDOB. Still, the *K* value for the 300-m shot is quite large and its SDOB is far greater than the most overburied NTS explosion that we have processed to date (~400). The measured *K* value for that explosion is 2.8. Therefore, *K* does systematically decrease over the range of SDOB between 400 and 1,500 scale meters and approaches 1. However, the persistence of tensile failure and size of *K* values for such large SDOBs are indeed surprising.

Could *K* increase over a range of SDOB between nominal values of 120 and values as large as 400-scale meters? Perhaps, and the reason might be related to the dynamics of spall slapdown, as was proposed above for the decrease in *K* of very large Pahute Mesa explosions. Spallation is significantly weaker over ground-zero on overburied explosions compared to normal-buried explosions. Therefore, the impulse of slapdown should not cause a proportional amount of compaction as it does for normal buried explosions, especially at depths where the effects of cavity rebound are the strongest (App and Brunish, 1992), and the coupling of the CLVD source into the ground for NTS explosions is the best. Consequently, M_{CLVD} might be proportionately greater for overburied explosions, at least for an intermediate range of SDOB above which mechanisms of deep-seated tensile failure should begin to “shut off” significantly, and *K* values decrease. Hydrodynamic simulations to test such hypothesis would be extremely valuable.

After better measurements from moment-tensor inversions become available, correlation studies will try to determine causes of variability in *K* in terms of emplacement conditions and material properties. Our ultimate goal is to develop a model to explain *S*-wave generation from explosions, and some preliminary signs suggest that shock-induced, deep-seated tensile failure does indeed play a role, as discussed in the next paragraph.

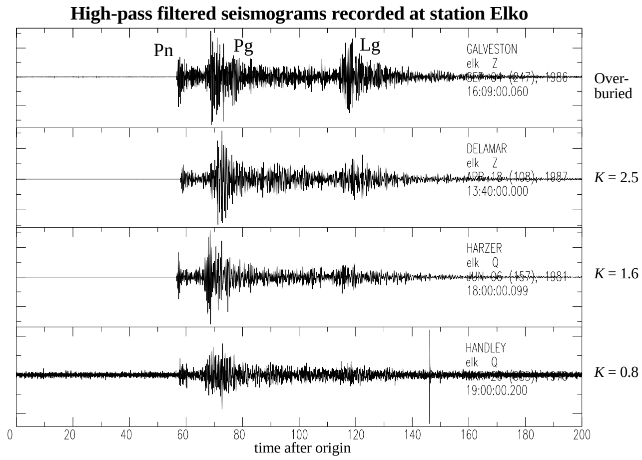

Figure 3. Butterworth-filtered seismograms using 4-poles, and 1-pass, with a corner frequency of 2 Hz.

It is well-known that large-magnitude explosions discriminate extremely well using high-frequency *P/S* ratios. Taylor (1995) was among the first to note, "...that large NTS explosions ($m_b > 6$) are characterized by the largest *Pg/Lg* ratios and are similar to signals expected for pure explosions." This is interesting in light of what was discussed about the yield dependence of *K*, where inferred and measured values approach 1.0 or less for large Pahute Mesa explosions. Following Taylor (1995), I made a cursory look at some high-frequency signals recorded at the Livermore network station ELKO about 400 km from Pahute Mesa. These signals are shown in Figure 3, where 3 of the 4 shots have estimates of *K* and the fourth is an over-buried explosion. While the *K* value has not been measured for this test, its SDOB is similar to Rainier Mesa explosions that have the largest *K* values measured to date. Figure 3 shows that the amplitudes of *Lg* waves compared to the *P* phases are dramatically different for Handley (m_b 6.4) and Galveston (m_b 3.7). Once better measurements of *K* are available for more NTS explosions, correlation studies will also investigate the dependence of *P/S* ratios on *K*.

Inferred K for STS explosions. *K* values for nuclear explosions at the Semipalatinsk Test Site (STS) will be inferred in the same way they were for NTS. Comparisons between *K* values for NTS and STS explosions are important to do because there are several expectations based on the model of shock-induced, deep-seated tensile failure.
(1) *K* values should be larger at STS on average. STS explosions are buried shallower for their yield compared to NTS explosions. Also, the mechanism of shear dilatancy plays a more significant role in hard rock media (Heuzé et al., 1991), and that should make *K* larger too. For some explosions, *K* values could become large enough for the CLVD to reverse the polarity of the *A* spectrum.
(2) *K* should not show as much yield dependence at STS. We posit that the reduction in *K* for NTS explosions is due to (a) compacting gas-filled pores in the media above the water table and (b) crushing displaced blocks that have been heaved upward by cavity rebound beneath the spall-parting depth. Both of these effects occur when the impulse of slapdown exceeds the strength of the tuff matrix. Since spall impulse increases with yield, *K* is expected to decrease as yield increases. On the other hand, there is essentially zero gas-filled porosity for STS explosions, and the granite matrix is stronger.

Ekström and Richards (1994; ER94) measured gain factors for the *A* spectrum on 71 nuclear explosions located at the Balapan test area. These gain factors, which they call U_1, are provided in Table 1 of their paper. To compare NTS results with those of EK94, the units of U_1 and of the abscissa in Figure 1 of this paper must be on a common scale. This common scale will be seismic moment in units of 10^{15} *Nm*. The relationship between U_1 and logA' can be ascertained by noting that $A(\omega) = 2U_1 \cdot G_1(\omega)$. ER94 state on p. 133 of their paper that U_1 must be multiplied by 9.46 to convert into units of 10^{15} *Nm*. The seismic moment of the template *A* spectrum for NTS was determined to be 6.5×10^{15} *Nm*. Thus the results in ER94 are related to the abscissa in Figure 1 by the formula $6.5 \cdot A' = 2 \cdot U_1$, where U_1 has been multiplied by 9.46.

It is interesting to note that ER94 finds that 8 of the 71 tests have negative U_1 values, indicating that the *A* spectra for these STS explosions have reverse polarities. Reversed polarity *A* spectra have not been observed on NTS tests, and these facts suggest that the K values for these 8 explosions are significantly larger than measurements of K for NTS explosions, just as anticipated in (1) above.

Figure 4 shows a plot of NTS and STS observations similar to the plot in Figure 1 except that the abscissa is now in terms of seismic moment in units of 10^{15} Nm. Plotted are just those STS explosions with normal polarity. The m_b's are taken from Ringdal *et al*. (1992) and are based on the work of Blacknest seismologists. A subset of NTS observations in Figure 1, consisting of 29 shots above the water table on Pahute Mesa, are plotted for comparison. It is evident that the scatter is considerably larger for STS observations than it is for this subset of NTS shots. Indeed, the scatter of NTS observations is relatively small over the entire yield range in Figure 1.

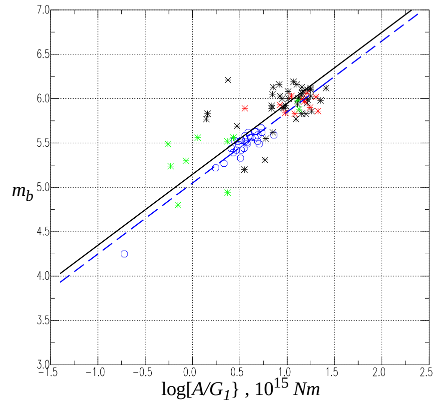

Figure 4. *A*-spectrum gain factor plotted against m_b for NTS and STS explosions. NTS gain factors and line fit are blue circles and a dashed line. The STS gain factors are color-coded by test area (NE, TZ, and SW), and the fit is a solid black line.

The lines in Figure 4 are fits to the observations under the constraint that the slope equals 0.8. This value of slope was chosen because compilations of m_b - M_s observations support relationships of the form $M_s = 1.25m_b - B$ for NTS and STS, where B is a constant (Murphy, 2005). Clearly, the scatter of STS observations does not justify a quadratic fit used for NTS observations in Figure 1, and the subset of 29 explosions is adequately fit by a linear equation.

Using a linear approximation, we can write the following

$$m_b = L_1 \cdot \log[A/G_1] + L_2 \tag{7}$$

and

$$m_b = m_1 \cdot \log W + m_2 \ . \tag{8}$$

L_1 is constrained to equal 0.8, and L_2, m_1, and m_2 are free parameters determined from regressions. Plugging formulas for log[A/G_1] (Equation 5) and m_b into Equation 7, substituting for M_I using the equations in DJ91, and then solving for the index K yields

$$K = \frac{2(1-\nu) \cdot (3-\Im)}{\Im + \nu(6-\Im)} \tag{9}$$

where $\Im = 10^{F_2} \cdot W^{F_1}$, (10)

$$F_1 = 0.4385a + [(m_1 - L_1)/L_1] \ , \tag{11}$$

and F_2 is a function of density, velocity, Poisson ratio ν, gas-filled porosity of the source medium, h_o, and parameters L_1, L_2, and m_2. Depth of burial follows the scaling rule $h = h_o \cdot W^a$ in meters.

It can be shown that K must decrease with yield if F_1 is positive. F_1 is a function of the exponent a and the yield scaling parameter m_1. The 1-Hz P waves from NTS and STS explosions do not yield scale similarly: an m_1 value of ~0.9 is generally found for NTS (Vergino and Mensing, 1990), and for STS, the value is ~0.75 (Ringdal et al., 1992).

Using these nominal values for m_1, the inferred yield scaling exponent F_1 for explosions at the two test sites and for two different containment rules are summarized in Table 1 below.

Table 1: F_1 for NTS and STS Explosions Based on Different Containment Rules

a	NTS	STS
1/4	0.235	0.047
1/3	0.271	0.084

F_1 is found to be positive for NTS, as we expected, and the same is true for STS, although it is much smaller. Thus, K will decrease with yield at both test sites. The rate of decrease depends not only on the exponent F_1 but also on the size of the coefficient, 10^{F_2}. Using nominal values for density, velocity, and gas porosity for the test sites, a ν of 1/4, h_o and m_2 values of 100 and 4.45 for STS, and L_2 values of 5.05 and 5.15 from the fits in Figure 4, the coefficients on $\Im$ equal 0.21 and 0.30 for NTS and STS, respectively. Assuming cube-root containment practice, the inferred K values are 1.65 and 2.1 for 100-*kt* explosions at NTS and STS. The rate at which K decreases is lower for STS than it is for NTS. If the containment practice at STS is quarter-root, the rate of decrease is even less. These results are consistent with the expectations based on the physical model discussed at the beginning of this sub-section.

CONCLUSIONS AND RECOMMENDATIONS

The first year of this project has witnessed good progress toward developing a new analytical explosion source model that will account for the generation of *P* and *S* waves. The model is built upon spherical source models developed almost 40 years ago, which served the monitoring community well but are recognized to be inadequate to explain *S*-wave generation. Our approach in developing a new model is to start with a long-period description, and future work will add increasing complexity to the source description in order to explain more observations for higher frequencies. To date, some interesting discoveries have been made from long-period predictions of the model:

(1) Interference between Rayleigh waves excited by the monopole and the CLVD, which is the kinematic representation of shock-induced, deep-seated tensile failure, reduces M_s making explosions look more explosion-like on plots of m_b - M_s.

(2) m_b - M_s observations for the North Korean test of 9 October 2006 can be explained if there was suppression of tensile failure. Indeed, this test may be one of the few examples of a source that is purely explosive with no significant secondary sources. Patton and Taylor (2008) show that its m_b - M_s observations are consistent with the MM71 model, while MM71 cannot explain m_b - M_s for the vast majority of other tests conducted worldwide.

(3) A long-period measure of the relative strength of tensile failure, K, decreases with yield for NTS explosions. The phenomenology of tensile failure and causes of the decrease suggest that K for STS explosions should be larger on average than NTS explosions and should show less decrease with yield. Preliminary results appear to support both predictions.

ACKNOWLEDGEMENTS

I have benefitted over the year from many helpful discussions and email exchanges with Dr. Steven R. Taylor.

REFERENCES

App, F. N., and W. M. Brunish (1992). Modelling surface motion and spall at the Nevada Test Site, *LA-UR-92-0500*, Los Alamos National Laboratory Report, Los Alamos, NM.

Denny, M. D., and L. R. Johnson (1991). The explosion seismic source function: Models and scaling laws reviewed, in *Explosion Source Phenomenology, AGU Monograph, 65*, edited by S. Taylor, H. Patton, and P. Richards, 1–24.

Ekström, G., and P. G. Richards (1994). Empirical measurements of tectonic moment release in nuclear explosions from teleseismic surface waves and body waves, *Geophys. J. Int.* 117: 120–140.

Heuzé, F. E., T. R. Butkovich, O. R. Walton, and D. M. Maddix (1991). Explosion Phenomenology in jointed rocks: New insights, in *Explosion Source Phenomenology*, *AGU Monograph*, 65, edited by S. Taylor, H. Patton, and P. Richards, 253–260.

Mueller, R. A., and J. R. Murphy (1971). Seismic characteristics of underground nuclear detonations, Part I. Seismic spectrum scaling, *Bull. Seismol. Soc. Am.* 61: 1675–1692.

Murphy, J. R. (2005). Initial development of the IDC M_s/m_b event screening criteria, IDC Technical Experts Meeting on Event Screening, Arlington, VA, October.

Patton, H. J. (1988). Source models of the Harzer explosion from regional observations of fundamental-mode and higher-mode surface waves, *Bull. Seismol. Soc. Am.* 78: 1133–1157.

Patton, H. J. (1990). Characterization of spall from observed strong ground motions on Pahute Mesa, *Bull. Seismol. Soc. Am.* 80: 1326–1345.

Patton, H. J. (1991). Seismic moment estimation and the scaling of the long-period explosion source spectrum, in *Explosion Source Phenomenology*, *AGU Monograph, 65*, edited by S. Taylor, H. Patton, and P. Richards, 171–183.

Patton, H. J., J. L. Bonner, and I. N. Gupta (2005). Rg excitation by underground explosions: insights from source modelling the 1997 Kazakhstan depth-of-burial experiment, *Geophys. J. Int.* 163: 1006–1024.

Patton, H. J., and S. R. Taylor (2008). Effects of shock-induced tensile failure on m_b - M_s discrimination: Contrasts between historic nuclear explosions and the North Korean test of 9 October 2006, *Geophys. Res. Lett*. 35: L14301, doi:10.1029/2008GL034211.

Ringdal, F., P. D. Marshall, and R. W. Alewine (1992). Seismic yield determination of Soviet underground nuclear explosions at the Shagan River test site, *Geophys. J. Int. 109*: 65–77.

Romanowicz, B. A. (1982). Moment tensor inversion of long-period Rayleigh waves: A new approach, *J. Geophys. Res.* 87: 5395–5407.

Taylor, S. R. (1995). Problems associated with *Pg/Lg* ratios from NTS explosions affecting seismic discrimination, Los Alamos National Laboratory Report LA-UR-95-3635, Los Alamos, NM.

Toksöz, M. N., and H. H. Kehrer (1972). Tectonic strain release by underground nuclear explosions and its effect on seismic discrimination, *Geophys. J. R. Astr. Soc.* 31: 141–161.

Vergino, E. S., and R. W. Mensing (1990). Yield estimation using regional $m_b(Pn)$, *Bull. Seismol. Soc. Am.* 80: 656–674.